




Review

Assessing the Impact of Agents with Antiviral Activities on Transmembrane Ionic Currents: Exploring Possible Unintended Actions

Geng-Bai Lin ^{1,†}, Chia-Lung Shih ^{2,†}, Rasa Liutkevičienė ³, Vita Rovite ⁴, Edmund Cheung So ⁵, Chao-Liang Wu ⁶
and Sheng-Nan Wu ^{7,8,*}

¹ Division of Critical Care Medicine, Department of Surgery, Ditmanson Medical Foundation Chia-Yi Christian Hospital, Chia-Yi City 600566, Taiwan; shoubai2006@gmail.com

² Clinical Research Center, Ditmanson Medical Foundation Chia-Yi Christian Hospital, Chia-Yi City 600566, Taiwan

³ Neuroscience Institute, Lithuanian University of Health Sciences, LT-44307 Kaunas, Lithuania; rliutkeviene@gmail.com

⁴ Latvian Biomedical Research and Study Centre, LV-1067 Riga, Latvia; vita.rovite@biomed.lv

⁵ Department of Anesthesia, An Nan Hospital, China Medical University, Tainan 70965, Taiwan; edmundsotw@gmail.com

⁶ Ditmanson Medical Foundation Chia-Yi Christian Hospital, Chia-Yi City 600, Taiwan; wumolbio@mail.ncku.edu.tw

⁷ Department of Research and Education, An Nan Hospital, China Medical University, Tainan 70965, Taiwan

⁸ School of Medicine, College of Medicine, National Sun-Yat-Sen University, Kaohsiung 80421, Taiwan

* Correspondence: 071320@tool.caaumed.org.tw; Tel.: +886-6-3553111-3657

† These authors contributed equally to this work.

Abstract: As the need for effective antiviral treatment intensifies, such as with the coronavirus disease 19 (COVID-19) infection, it is crucial to understand that while the mechanisms of action of these drugs or compounds seem apparent, they might also interact with unexplored targets, such as cell membrane ion channels in diverse cell types. In this review paper, we demonstrate that many different drugs or compounds, in addition to their known interference with viral infections, may also directly influence various types of ionic currents on the surface membrane of the host cell. These agents include artemisinin, cannabidiol, memantine, mitoxantrone, molnupiravir, remdesivir, SM-102, and sorafenib. If achievable at low concentrations, these regulatory effects on ion channels are highly likely to synergize with the identified initial mechanisms of viral replication interference. Additionally, the immediate regulatory impact of these agents on the ion-channel function may potentially result in unintended adverse effects, including changes in cardiac electrical activity and the prolongation of the QTc interval. Therefore, it is essential for patients receiving these related agents to exercise additional caution to prevent unnecessary complications.

Keywords: antiviral agent; ion-channel modifier; ionic current; Na⁺ current; K⁺ current



Citation: Lin, G.-B.; Shih, C.-L.; Liutkevičienė, R.; Rovite, V.; So, E.C.; Wu, C.-L.; Wu, S.-N. Assessing the Impact of Agents with Antiviral Activities on Transmembrane Ionic Currents: Exploring Possible Unintended Actions. *Biophysica* **2024**, *4*, 128–141. <https://doi.org/10.3390/biophysica4020009>

Academic Editor: Danilo Milardi

Received: 4 January 2024

Revised: 26 January 2024

Accepted: 30 January 2024

Published: 27 March 2024



Copyright: © 2024 by the authors. Licensee MDPI, Basel, Switzerland. This article is an open access article distributed under the terms and conditions of the Creative Commons Attribution (CC BY) license (<https://creativecommons.org/licenses/by/4.0/>).

1. Introduction

An antiviral agent refers to a substance or medication used to treat viral infections or inhibit viral growth, replication, and dissemination within the body. These drugs or compounds are designed to target and disrupt the life cycle of viruses, thereby preventing them from infecting host cells or replicating. The agents with antiviral activities can be used to manage and treat a wide range of viral infections, including those caused by viruses such as hepatitis B and C, influenza, coronavirus disease 19 (COVID-19), and more [1,2]. However, in the context of various drugs or compounds employed to interfere in, prevent, or treat infections caused by different viruses, it has become evident that they possess significant regulatory effects on transmembrane ion channels located on the cell membrane. Using advanced patch-clamp technology in conjunction with precise voltage-clamping

profiles achieved through digital-to-analog conversions facilitates the accurate detection of distinctive ionic currents at the surface of various small cells [3,4]. Therefore, these alterations in ionic currents not only influence the normal functions of host cells but also assume a role in either exacerbating the progression of viral infections [5,6] or causing other adverse effects [7–10].

In this review paper, we provide descriptions of specific drugs or compounds that disturb viral replication while also exerting multiple regulatory effects on ion channels in cell membranes in various cell types. These agents are presented in alphabetical order. Table 1 showcases the two-dimensional chemical structure of each agent, while Table 2 outlines their abbreviations and documented effects on transmembrane ionic currents.

Table 1. Two-dimensional chemical structures of the drugs or compounds mentioned in this paper. The cell type studied and the concentration range used are illustrated. These data were obtained from PubChem (<https://pubchem.ncbi.nlm.nih.gov/>) (accessed on 4 October 2023).

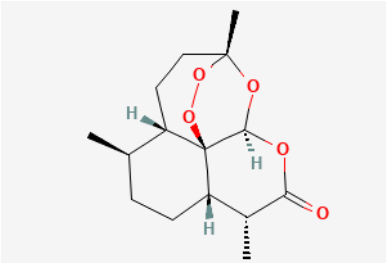
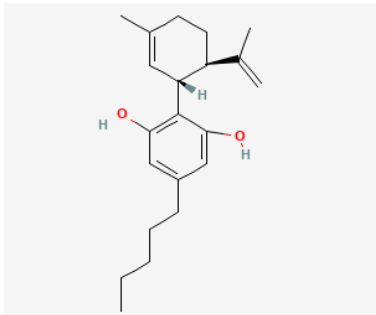
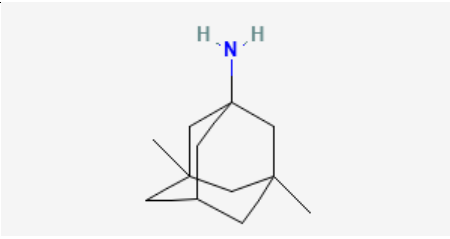
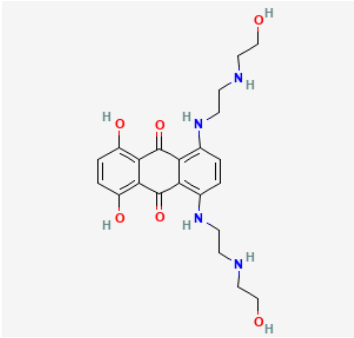
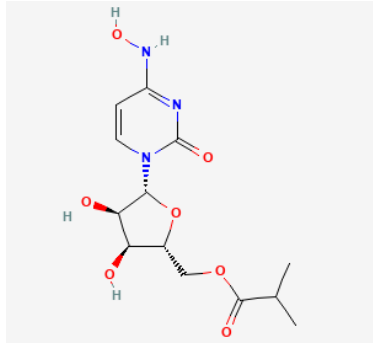
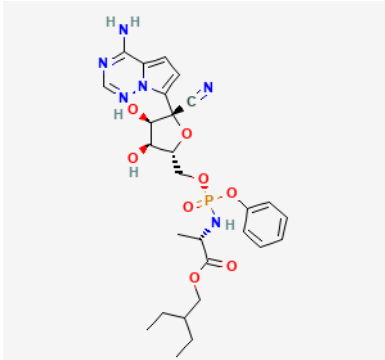
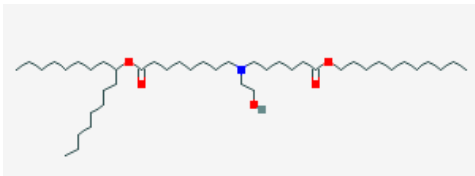
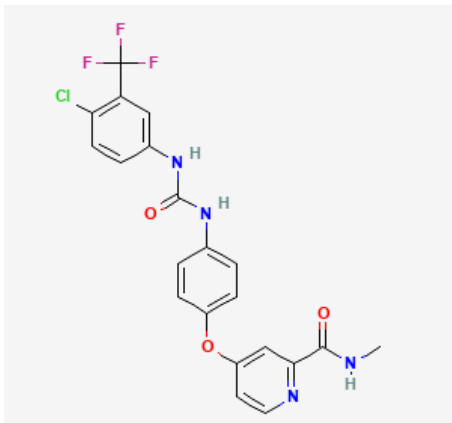
Compound or Drug	Chemical Structure	Cell Type Studied	Concentration Range Used
Artemisinin		GH ₃ cells, TRPC3-expressing HEK293 cells	1–100 μM
Cannabidiol		GH ₃ cells	0.3–100 μM
Memantine		GH ₃ , RAW 264.7, and BV2 cells	10–1 mM
Mitoxantrone		RAW 264.7 cells	1–100 μM

Table 1. Cont.

Compound or Drug	Chemical Structure	Cell Type Studied	Concentration Range Used
Molnupiravir	 The chemical structure of Molnupiravir consists of a pyrimidine ring system fused to a ribose sugar. The pyrimidine ring has a carbonyl group at the 2-position and a hydroxyl group at the 4-position. The ribose sugar is attached to the 5-position of the pyrimidine ring. The ribose sugar has hydroxyl groups at the 2' and 3' positions. A propanoic acid side chain is attached to the 4' position of the ribose sugar.	GH ₃ cells	1–300 μ M
Remdesivir	 The chemical structure of Remdesivir features a pyrimidopyrimidine ring system. The pyrimidine ring has a carbonyl group at the 2-position and a hydroxyl group at the 4-position. The pyrimidopyrimidine ring is attached to a ribose sugar. The ribose sugar has hydroxyl groups at the 2' and 3' positions. A phosphonate group is attached to the 4' position of the ribose sugar. The phosphonate group is further substituted with a phenyl ring and a propanoic acid side chain.	GH ₃ and Jurkat T cells	0.3–100 μ M
SM-102	 The chemical structure of SM-102 is a long-chain alkyl compound. It features a long hydrocarbon chain with several functional groups, including a primary amine, a secondary amine, and a tertiary amine, all of which are substituted with various groups.	GH ₃ cells and Leydig MA-10 cells	3–1 mM
Sorafenib	 The chemical structure of Sorafenib is a complex molecule. It features a central benzene ring with a chlorine atom and a trifluoromethyl group. This benzene ring is connected via an amide linkage to another benzene ring. This second benzene ring is further connected via an ether linkage to a pyridine ring. The pyridine ring has a carbonyl group and a methyl group attached to it.	H9c2, RUES2 cells *, and neonatal rat ventricular myocytes	1–30 μ M

* RUES2 cells refer to a human embryonic stem cell line that has undergone differentiation into cardiomyocytes.

Table 2. Drugs or compounds presented in this paper. These agents can potentially disrupt viral infections but may also impact various ionic currents.

Compound or Drug	Abbreviation	Actions on Ionic Currents *, **	References
Artemisinin	ART	↓ $I_{K(DR)}$ ↓ I_{Na} ↑ TRPC channel	Qiao et al. (2007) [11] So et al. (2017) [12] Zhang et al. (2022) [13]
Cannabidiol	CBD	↓ $I_{K(M)}$ ↓ I_h	Liu et al. (2023) [14]
Memantine	MEM	↓ I_{MEP} ↓ $I_{K(IR)}$	Wu et al. (2011) [15] Tsai et al. (2013) [16]
Mitoxantrone	MX	↓ $I_{K(IR)}$	Wang et al. (2012) [17]
Molnupiravir	MOL	↓ I_{Na}	Shiau et al. (2023) [18]
Remdesivir	RDV	↓ $I_{K(DR)}$ ↓ $I_{K(M)}$ ↑ I_{MEP} ↓ $I_{K(erg)}$	Chang et al. (2020) [19] Amarh et al. (2023) [20]
SM-102	SM-102	↓ $I_{K(erg)}$ ↓ $I_{K(IR)}$	Cho et al. (2021) [21]
Sorafenib	SOR	↓ $I_{K(erg)}$ ↓ $I_{K(S)}$ ↓ $I_{K(IR)}$	Wu et al. (2012) [22] Chang et al. (2020) [23]

* "↓" represents an inhibitory action on ionic current, while "↑" denotes a stimulatory action. ** Each of the ionic currents is presented in shorthand, with their corresponding full names listed in the Abbreviations Section.

2. Summary

The agents with antiviral activities known to exert regulatory effects on transmembrane ionic currents are illustrated in Figure 1.

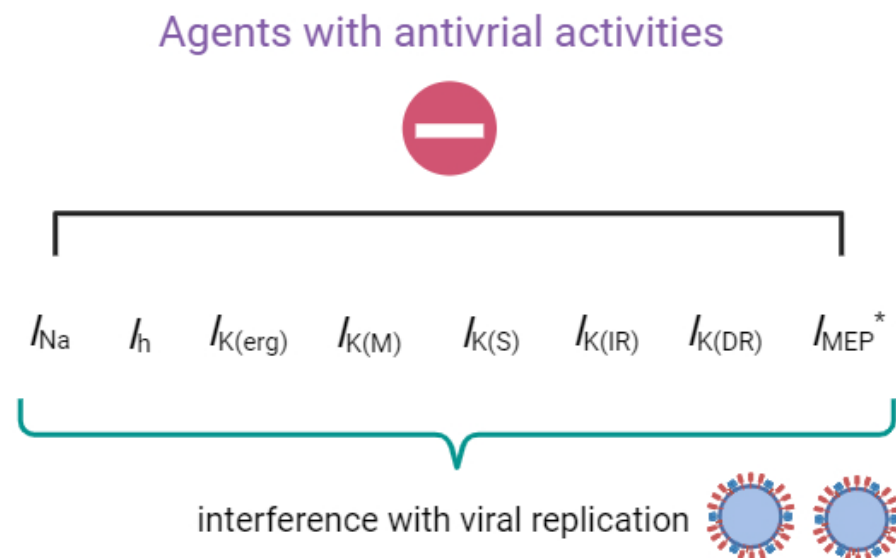


Figure 1. Graph demonstrating that upon exposure to the compounds or drugs described in this paper, their interactions with these ionic currents (e.g., I_{Na} , I_h , $I_{K(erg)}$, $I_{K(M)}$, $I_{K(S)}$, $I_{K(IR)}$, $I_{K(DR)}$, and I_{MEP}) will, in turn, interfere with the growth and replication of the virus. * indicates that I_{MEP} is stimulated by the presence of remdesivir (RDV).

2.1. Artemisinin (ART)

For centuries, ART (qinghaosu) has been widely acknowledged as a potent antimalarial agent. This remarkable compound is derived from the sweet wormwood plant, which is scientifically known as *Artemisia annua* L. It features a unique chemical structure characterized by a sesquiterpene trioxane lactone containing an unusual peroxide bridge [24]. Beyond its well-established antimalarial properties, ART exhibits a diverse range of pharmacological effects. These effects encompass cytotoxicity against tumor cells, along with antiviral and antiparasitic actions [24,25]. Moreover, recent research has unveiled its promising potential in combating the severe acute respiratory syndrome coronavirus 2 (SARS-CoV-2) [26,27].

Notably, previous reports have shown that artemisinin can synergistically act to suppress the delayed-rectifier K^+ current ($I_{K(DR)}$) and voltage-gated Na^+ current (I_{Na}) identified in pituitary tumor (GH₃) cells [12]. The inhibitory effect of ART on I_{Na} was also observed in nodose ganglion neurons [11]. Cell exposure to ART did not simply reduce the amplitude of $I_{K(DR)}$. It caused a significant increase in the $I_{K(DR)}$ inactivation rate elicited in response to a 10 s maintained depolarizing pulse. The IC_{50} is the concentration of the compound at which the biological response is reduced by 50%. The IC_{50} value, signifying the concentration of ART required to inhibit $I_{K(DR)}$, was 11.2 μ M, closely resembling the K_D value of 14.7 μ M obtained from the first-order binding scheme [12]. This value is typically interpolated from the concentration–response curve. It is commonly calculated using regression analysis. Exposure to ART caused a leftward shift in the midpoint of the steady-state inactivation curve of $I_{K(DR)}$, with no change in the curve's steepness. The presence of ART also enhanced the rate of excessive accumulative inactivation of $I_{K(DR)}$ evoked in response to repetitive stimuli. These results suggest that the ART-induced block of $I_{K(DR)}$ mainly occurred after channel opening. Prior to channel activation, the ART-binding site is likely to be either in a low-affinity state or inaccessible to the compound [12].

On another note, the presence of ART has the potential to engage in interactions with voltage-gated Na^+ (Na_V) channels. These interactions, in turn, lead to a decrease in both the peak amplitude of voltage-gated Na^+ current (I_{Na}) and the rate of inactivation of this current [12]. Consequently, the observed inhibition of I_{Na} and $I_{K(DR)}$ when ART is present could synergistically influence the functional activities of pituitary cells, provided that similar results are replicated in an *in vivo* context. The ability of ART to activate canonical transient receptor potential (TRP) channels, such as TRPC3 channels, has also been recently demonstrated [28].

Previous studies have demonstrated that ART effectively suppresses cell proliferation and hormonal secretion in various cell types, including GH₃ cells [29,30]. It is pertinent to investigate the extent to which the antiviral, neurological, or ototoxic effects induced by ART [24,25,29,30] are closely linked to its influence on ionic currents.

2.2. Cannabidiol (CBD)

CBD, scientifically referred to as 2-[(1R,6R)-3-methyl-6-prop-1-en-2-ylcyclohex-2-en-1-yl]-5-pentylbenzene-1,3-diol, is a non-psychoactive cannabinoid derived from the Cannabis plant renowned for its potential therapeutic applications [31]. In addition to its known attributes, recent research has highlighted CBD's role in hindering the entry of SARS-CoV-2, including its emerging variants, and its ability to exhibit antiviral effects against a wide range of viruses, both enveloped and non-enveloped [32,33]. Moreover, recent studies have shed light on CBD's capacity to modulate activity within the hypothalamic–pituitary–adrenal axis [34]. It has also been shown to influence various types of transmembrane ionic currents in electrically excitable cells, including I_{Na} and M-type K^+ current ($I_{K(M)}$) [35]. The biophysical and pharmacological characteristics of $I_{K(M)}$, a current encoded by KCNQ genes, have been established in previous studies [21,36,37]. Among KCNQ genes, KCNQ2 and KCNQ3 subunits heteromultimerize to form the channels responsible for $I_{K(M)}$ in neurons [37]. In recent research conducted on pituitary GH₃ cells, it was demonstrated that exposure to CBD leads to the suppression in the amplitudes of $I_{K(M)}$ and the hyperpolarization-activated cation current (I_h), with the corresponding IC_{50} values of 3.6 and 3.3 μ M, respectively [14]. The biophysical property of I_h

is distinctive, marked by its slow activation kinetics during sustained hyperpolarization [38,39]. Furthermore, given CBD's impact on ion channels situated on the cell membrane, it appears unlikely that these effects can be solely ascribed to CBD's interaction with cannabinoid receptors. Therefore, there is a significant demand for more comprehensive research to investigate the mechanisms through which CBD affects these ion channels. This regulation, whether it results in direct or indirect interference with virus attachment or cell entry into cells, demands further investigation. Similarly, to gain a clearer understanding of how CBD modulates ionic currents and its potential impact on specific downstream signaling pathways, further in-depth studies are warranted.

2.3. Memantine (MEM, Namenda®)

MEM (1-amino-3,5-dimethyladamantane), which is a derivative of amantadine, has found application in the management of neurological disorders characterized by excitotoxic cell death. This encompasses conditions such as Parkinson's disease and vascular dementia [40]. MEM has been reported to be repurposed against the Chikungunya virus or to ameliorate the symptoms of long coronavirus disease 19 (COVID-19) syndrome [41–43]. The therapeutic effect of MEM was previously thought to be due to its ability to bind preferentially to N-methyl-D-aspartate (NMDA) receptor-operated cation channels.

Despite NMDA receptors being the primary target for MEM, several studies reported additional underlying mechanisms of action. For example, previous work has demonstrated that MEM exerted a depressant action on membrane electroporation-induced inward current (I_{MEP}) in a concentration-dependent manner in pituitary tumor (GH₃) cells [15]. Membrane electroporation (MEP) is a well-established process known for significantly enhancing the electrical conductivity and permeability of the plasma membrane when subjected to an externally applied electrical field [44]. The electrical and pharmacological properties of I_{MEP} in both heart cells and pituitary cells have been previously demonstrated [15,22,45].

Additionally, previous research has demonstrated that the MEM presence reduces the amplitude of the inwardly rectifying K⁺ current ($I_{K(IR)}$) in both RAW 264.7 macrophages and BV2 microglial cells [16]. MEM exposure has been observed to decrease both the rate and extent of $I_{K(IR)}$ inactivation. Notably, the intracellular inclusion of spermine has been found to counteract the inhibitory effects of MEM on $I_{K(IR)}$. Spermine, a polyamine and polycationic compound, has been shown to block the inward rectifying K⁺ (Kir) channel [46]. Moreover, in single-channel recordings performed on RAW 264.7 cells, it was observed that MEM effectively decreased the open-state probability of the Kir channel while not affecting the single-channel conductance [16]. MEM-mediated reduction in Kir-channel activity was concomitant with both an increase in mean closed time and a decrease in the slow component of mean open time.

The Kir channels display strong inward rectification, meaning that they preferentially conduct K⁺ ions into the cell rather than out of the cell. Their gating mechanism is influenced by several factors, such as intracellular Mg²⁺ ions, polyamines, and phosphatidylinositol-4,5-bisphosphate [46]. The activity of these channels plays a crucial role in maintaining the resting membrane potentials of cells. They also contribute to the regulation of cell excitability, particularly in neurons and cardiac myocytes [46].

Consequently, it is expected that the reduction in $I_{K(IR)}$ magnitude caused by MEM may serve as a crucial mechanism by which MEM or similar compounds can disrupt the functional activities of macrophages or microglial cells, possibly contributing to their antiviral effects. However, these effects should be confirmed through further research in vivo.

2.4. Mitoxantrone (MX, Novantrone®)

MX (1,4-dihydroxy-5,8-bis[[2-[(2-hydroxyethyl)amino]ethyl]amino]anthracene-9,10-dione) is a synthetic anthracenedione that has firmly established itself as an antineoplastic agent. It achieves this status by intercalating with DNA, thereby impeding the function of the topoisomerase II enzyme, preventing the ligation of DNA strands, and ultimately delaying cell-cycle

progression. The therapeutic potential of MX has extended to a wide spectrum of malignancies, including advanced cases of prostate and breast cancers with osseous metastasis [47]. Furthermore, MX exhibits efficacy in countering viral infections, operating through similar mechanisms that disrupt viral DNA or RNA replication [48].

Earlier reports have shown that the presence of MX interacts with the activity of Kir channels to suppress the magnitude of $I_{K(IR)}$ in osteoclast precursor RAW 264.7 cells differentiated with lipopolysaccharide [17]. MX inhibits the amplitude of $I_{K(IR)}$ in a concentration-dependent manner, with an IC_{50} value of 6.4 μ M. Doxorubicin or tertiapin also effectively suppresses the $I_{K(IR)}$ amplitude. Doxorubicin is another anthracycline compound, while tertiapin, a bee venom peptide, has been described as an inhibitor of acetylcholine-activated K^+ current and $I_{K(IR)}$ in heart cells [49]. The MX-mediated decrease in Kir-channel activity is also accompanied by the shortening of the mean open time of the channel [17]. Blocking Kir channels in osteoclasts could hold significant clinical potential for the treatment of disorders characterized by disrupted mineralized tissues [50]. The suppression of these channels can also contribute to viral infections, such as the Monkeypox virus infection [48].

2.5. Molnupiravir (MOL, EIDD-2801, MK-4482, Lagevrio®)

MOL, an orally administered small-molecule isopropylester prodrug, is a noteworthy representative of the ribonucleoside analog β -d-N4-hydroxycytidine. This synthetic compound is esteemed for its antiviral properties, effectively hampering the replication of specific RNA viruses by inducing critical errors during viral RNA replication processes [51,52]. Its chemical nomenclature designates it as ((2R,3S,4R,5R)-3,4-dihydroxy-5-(4-(hydroxyamino)-2-oxopyrimidin-1(2H)-yl) tetrahydrofuran-2-yl) methyl isobutyrate. In light of its capacity to thwart the RNA-dependent RNA polymerase (RdRp) of SARS-CoV-2, consequently prompting RNA mutagenesis, MOL has been repurposed as a potential treatment for COVID-19 [53].

In a recent study, researchers presented findings demonstrating that MOL exerts a time-, concentration-, and frequency-dependent inhibition of I_{Na} in pituitary tumor (GH₃) cells [18]. Upon exposure to MOL, both the peak and late amplitudes of I_{Na} in response to rapid membrane depolarization experienced varying degrees of suppression. The study estimated the IC_{50} values of MOL for inhibiting transient and late I_{Na} in GH₃ cells to be 26.1 and 6.3 μ M, respectively. Furthermore, MOL's continuous presence led to cumulative inhibition of peak I_{Na} elicited throughout a series of depolarizing stimuli. Additionally, the introduction of MOL substantially attenuated the nonlinear resurgent I_{Na} evoked by the descending ramp voltage, highlighting its impact on specific electrophysiological responses. The magnitude of resurgent I_{Na} plays a crucial role in triggering action potential firing in different types of electrically excitable cells. In the presence of MOL, single-channel recordings showed a reduction in the probability of Na_V-channel openings accompanied by a decrease in the mean open time of the channel; however, no change in single-channel conductance was made [18]. The voltage-activated I_{Na} detected in Neuro-2a neuroblastoma cells was also found to be responsive to inhibition by MOL [54]. It has been reported that mRNA transcripts of NaV1.1, NaV1.2, and NaV1.6 α subunits are expressed in GH₃ cells [51]. It remains to be studied whether MOL can exert an influence on the activity in other isoforms of the Na_V channel.

The molecular docking analysis revealed potential interactions between MOL and the RdRp of SARS-CoV-2 and NaV channels [18]. Furthermore, recent studies have linked long-term MOL usage to the emergence of additional mutations in the SARS-CoV-2 genomes [52]. Whether these unintended side effects are related to its inhibition of I_{Na} warrants further investigation. Given that ranolazine is employed in the treatment of chronic angina pectoris [55], it is worthwhile to explore the potential repurposing of MOL for the management of chronic pain [54,56].

2.6. Remdesivir (RDV, GS-5734)

RDV (ethyl (2S)-2-[[[(2S,3S,4R,5R)-5-(4-aminopyrrolo[2,1-f][1,2,4]triazin-7-yl)-5-cyano-3,4-dihydroxyoxolan-2-yl]methoxy-phenoxy-phosphoryl]amino]propanoate), a potent antiviral agent with broad-spectrum activity, is acknowledged as a mono-phosphoramidate prodrug of an adenosine analog. It undergoes metabolic conversion into its active form, GS-441524, which is a C-adenosine nucleoside analog [57]. This compound, functioning as a nucleotide-analog inhibitor of RdRp, demonstrates substantial effectiveness against various coronaviruses (CoVs), including MERS-CoV, SARS-CoV-2, and the virus responsible for COVID-19 [58–62]. It stands out as a promising antiviral drug with potential applications against a wide spectrum of RNA viruses, primarily by targeting the viral RdRp. The active form, GS-441524, to which RDV metabolizes, exerts a less inhibitory effect on cellular RNA compared with its impact on viral polymerase [23]. Recent studies have unveiled the high efficacy of RDV in combination with chloroquine or hydroxychloroquine for controlling SARS-CoV-2 infection in in vitro settings [23]. Moreover, there is noteworthy ongoing research regarding the efficacy of RDV in treating SARS-CoV-2 infection in humans [63].

It is worth noting that prior investigators have revealed that the presence of RDV leads to a reduction in the amplitude of $I_{K(DR)}$ in a manner that is both time-dependent and concentration-dependent. This effect has been observed in both pituitary GH₃ cells and Jurkat T-lymphocytes [19]. Additionally, the rate of $I_{K(DR)}$ inactivation appears to increase with higher RDV concentrations. According to data from a simplified reaction model, the dissociation constant (K_D) required for RDV-induced inhibition of $I_{K(DR)}$ in GH₃ cells was reported to be approximately 3.04 μ M. This value is in close proximity to the effective IC₅₀ value (2.8 μ M) for the RDV-mediated suppression of sustained $I_{K(DR)}$, although it is lower than that of the IC₅₀ (10.1 μ M) for blocking the initial peak $I_{K(DR)}$. The exposure to RDV also suppressed the magnitude of $I_{K(M)}$, with an IC₅₀ value of 2.5 μ M in GH₃ cells, as well as depressed the voltage-dependent hysteresis of $I_{K(M)}$ [23].

Furthermore, under sustained exposure to RDV, it is noteworthy that neither the addition of α,β -methylene-ATP (AMPCPP), a non-degradable ATP analog, nor the introduction of 8-cyclopropyl-1.3-dipropylxanthine (DPCPX), an antagonist of the adenosine A₁ receptor, had any discernible impact on the inhibition of $I_{K(DR)}$ induced by RDV [64,65]. These results suggest that the altered magnitude of $I_{K(DR)}$ caused by RDV in GH₃ cells is unlikely to be associated with its preferential binding to purinergic or adenosine receptors. This observation is significant, particularly considering that the RDV molecule was initially considered a prodrug of an adenosine nucleoside analog [57,66]. Exposure to RDV was recently discovered to reduce the amplitude of $I_{K(erg)}$ [20] and also to prolong QTc intervals [64]. Nonetheless, the direct suppression of $I_{K(DR)}$, $I_{K(M)}$, and $I_{K(erg)}$ in these cells, therefore, suggests that this compound, per se, presumably is not an inactive prodrug. Moreover, the RDV presence can activate the magnitude of I_{MEP} [19].

It needs to be mentioned that prior studies have documented the presence of hypokalemia and, in some severe cases, lethal arrhythmia in patients with COVID-19 infection [60,65,67]. The EC₅₀ value of RDV against SARS-CoV-2 within Vero E6 cells was significantly determined to be 1.76 μ M, indicating that the concentration required for its antiviral action is likely attainable in an in vivo setting [61]. It is therefore anticipated that, apart from its effects on the viral polymerase and the proofreading exoribonuclease [57,62,66,68], the extent to which RDV-induced perturbations on ionic currents may participate in its antiviral actions has yet to be further delineated.

2.7. SM-102

SM-102, with its complex chemical name heptadecan-9-yl 8-((2-hydroxyethyl)(6-oxo-6-(undecyloxy)hexyl)amino)octanoate, 4-hydroxybutyl)azanediyl)bis(hexane-6,1-diyl)bis(2-hexyldecanoate, stands as a synthetic and ionizable amino lipid. It has found extensive application alongside other lipids in the formulation of lipid nanoparticles [69–71]. These formulations incorporating SM-102 have been notably instrumental in the creation of lipid nanoparticles for delivering mRNA-based vaccines. This highly efficient transfection

method relies on compacted lipopolyamine-coated plasmids and has seen progressive improvements over time [13,72]. However, it is important to note that recent reports have linked COVID-19 vaccinations to instances of myocarditis [73–77]. After receiving COVID-19 mRNA vaccination, there have been reported cases of acute myocarditis [74,75].

In a recent study, it was observed that, at concentrations of 100 or 300 μM , SM-102 caused a decrease in the amplitude of $I_{K(\text{erg})}$ and an elevation in the deactivation rate of the current in both GH₃ cells and Leydig MA-10 cells [78]. The inclusion of SM-102 resulted in a decrease in both the magnitude of $I_{K(\text{erg})}$ and a shift in the current-to-voltage relationship of sustained $I_{K(\text{erg})}$ towards less negative potentials. Additionally, the exposure of cells to SM-102 effectively reduced the magnitude of the voltage-dependent hysteretic strength of $I_{K(\text{erg})}$ when activated by an isosceles-triangular ramp voltage.

In GH₃ cells subjected to dialysis with SM-102, TurboFectinTM, or spermine, there was a gradual reduction in the magnitude of $I_{K(\text{erg})}$ [78]. TurboFectinTM is a proprietary blender of a wide-ranging protein/polyamine mixture, along with histones and lipids, designated as a known transfection reagent [79]. The sensitivity of $I_{K(\text{IR})}$ in microglial BV2 cells to suppression was also observed when exposed to SM-102 or spermine, as reported previously [16,78]. The extent to which SM-102-induced changes in membrane ionic currents contribute to the adverse effects of mRNA-based vaccines, such as ModernaTM, requires further investigation. An earlier report found that an individual experienced long QTc interval and syncope after receiving a single dose of COVID-19 vaccination [80]. It is, therefore, essential to determine whether the concentrations of SM-102 or TurboFectinTM used for directly altering ionic currents could be achieved in both in vitro and in vivo settings.

2.8. Sorafenib (SOR, Nexavar[®])

SOR, scientifically designated as 4-(4-(((4-chloro-3-(trifluoromethyl)phenyl)amino)carbonyl)phenoxy)-N-methylpyridine-2-carboxamide, belongs to a distinctive class of multi-targeted, active small-molecule tyrosine kinase inhibitors that are presently employed in the treatment of hematological and oncological malignancies. Strategies for dose escalation have been contemplated for their clinical use, given that many malignancies are believed to be instigated by aberrant tyrosine kinase activity [81]. Tyrosine kinase inhibitors, such as sunitinib and SOtR, have recently been noticed to exert antiviral action [82–84]. A previous report has demonstrated the ability of SOR to suppress the amplitude of both the slowly activating delayed-rectifier K⁺ current ($I_{K(S)}$) and $I_{K(\text{erg})}$ identified in H9c2 cardiomyocytes [19,22]. The K_V7.1-type $I_{K(S)}$, known as the K_V7.1 (or KCNQ1)-cloned K⁺ channel, has been noted to be suppressed during H9c2-cell exposure to SOR. Additionally, it is worth noting that the suppression of $I_{K(S)}$ caused by SOR takes time to manifest during long-lasting membrane depolarization and is not an instantaneous response upon channel opening. These findings thus imply the existence of a time-dependent binding site for SOR, possibly situated in or near the $I_{K(S)}$ -channel pore, specifically when the channel becomes active. The SOR presence likewise resulted in a reduction in the amplitude of $I_{K(\text{IR})}$, as observed in neonatal rat ventricular myocytes. This inhibition of ionic currents during SOR exposure may constitute an unintended yet crucial mechanism, contributing to alterations in QTc intervals or possibly influencing antiviral effects [9,19,82–84]. These findings could offer insights into the occurrence of patients exhibiting QTc prolongation and, in some cases, experiencing subsequent fatal arrhythmias following treatment with SOR [10,85].

3. Conclusions

It is acknowledged that viruses lack a complete cellular membrane structure and are not considered living organisms. They require a host cell to replicate, which necessitates their initial contact with the membrane of an infected cell. Therefore, when these antiviral medications discussed here are able to affect transmembrane ion channels in that cell, it can potentially disrupt the virus's attachment, insertion, and entry into host cells (Figure 1). However, it should be noted that most of the experimental observations are derived from tumor cell lines, such as GH₃ cells, neuroblastoma N2a cells, microglial BV2 cells, and RAW 264.7 macrophages. Further

research is, therefore, needed to determine the applicability of these findings to different types of native excitable cells *in vivo*. Alternatively, whether there is specificity in their action on ion channels linked to antiviral activity and whether it exhibits selectivity for anti-SARS-CoV-2 activity still warrant further investigation. While certain antiviral agents influence ionic currents with low selectivity, the highlighted off-target effects are crucial considerations for disease treatment. Alternatively, further investigation is required to determine the impact of ion channel modulation by agents with antiviral activities on practical outcomes or consequences at various stages of disease development or maintenance over time.

We also need to clarify that certain antiviral agents mentioned in this paper are indeed clinically approved for use. These drugs, such as remdesivir (RDV), have been reported to intervene in transmembrane ion currents. However, substances such as cannabidiol (CBD) or artemisinin (ART), while exhibiting antiviral activity, are inappropriately classified as antiviral agents. Additionally, ART is an antimalarial drug.

It is also important to emphasize that the majority of the ion currents highlighted in Figure 1 are observed on the cardiac cell membrane. If the concentrations used in this context were to influence cardiac cells, it could disrupt their electrical activity, possibly resulting in the prolongation of ventricular action potential and QTc interval (Figure 2) [65,85,86]. It could thus pose a significant risk of causing severe arrhythmias, such as torsade de pointes arrhythmia, or even sudden cardiac death [7–10,64,67,85,86]. These antiviral suppressants display a diverse array of chemical structures (Table 1) and exhibit various regulatory effects on manifold types of ionic currents (Table 2). Therefore, when it is indeed necessary to use antiviral therapies, it is essential to exercise caution and closely monitor to mitigate unforeseen events [7,8,10,67,87]. Although a thorough examination of electrophysiological studies was conducted with these antiviral agents, further investigation is required to determine the extent of specific focus on organs that bear significance in terms of ion channel functionality. Moreover, whether these agents with antiviral activities also affect the transcriptional or translational expression levels of these ion channels is worth further investigation in the future.

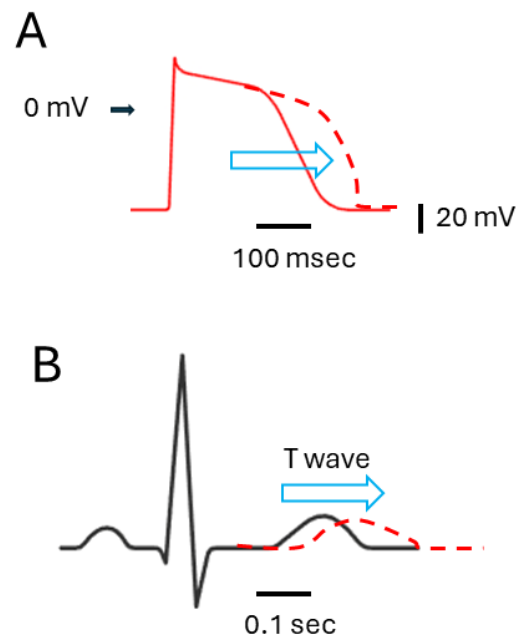


Figure 2. Impact of agents with antiviral activities on $I_{K(erg)}$ or $I_{K(S)}$ inhibition, and their influence on ventricular action potential ((A), red) and electrocardiogram ((B), black). The arrowhead on the left side of (A) indicates the 0 mV level. The horizontal and vertical black bars in the bottom right corner of (A,B) represent time and voltage scales, respectively. The red dashed curve in (A,B) illustrates the potential effects (denoted using horizontal blue open arrowheads) of these agents, specifically the prolongation of ventricular action potential (A) and QTc interval (B), respectively.

Author Contributions: Conceptualization, S.-N.W., R.L., V.R., E.C.S. and G.-B.L.; methodology, S.-N.W.; software, C.-L.W.; validation, G.-B.L., C.-L.S. and S.-N.W.; writing—original draft preparation, G.-B.L., and C.-L.S.; writing—review and editing, R.L., V.R., E.C.S. and C.-L.W.; visualization, G.-B.L.; supervision, S.-N.W.; funding acquisition, G.-B.L., C.-L.S. and S.-N.W. All authors have read and agreed to the published version of the manuscript.

Funding: This work was partly aided by the grants from the Ministry of Science and Technology (NSTC-110-2320-B-006-028, NSTC-111-2320-B-006-028, and NSTC-112-2923-B-006-001) and from An Nan Hospital (ANHRF-111-10, ANHRF-112-42, ANAR-112-43, and ANHRF-112-44), Taiwan. The funders of this study did not participate in the study design, data collection, analyses, or interpretation.

Institutional Review Board Statement: Not applicable.

Informed Consent Statement: Not applicable.

Data Availability Statement: Not applicable.

Acknowledgments: While there is a wealth of relevant papers that could be cited, we regret that, due to space limitations, we are unable to include all of them in this paper.

Conflicts of Interest: The authors declare no conflicts of interest.

Abbreviations

I_h	hyperpolarization-activated cation current
$I_{K(erg)}$	<i>erg</i> -mediated K^+ current
$I_{K(IR)}$	inwardly rectifying K^+ current
$I_{K(M)}$	M-type K^+ current
$I_{K(S)}$	slowly activating delayed-rectifier K^+ current
I_{MEP}	MEP-induced inward current
I_{Na}	voltage-gated Na^+ current
Kir channel	inwardly rectifying K^+ channel
MEP	membrane electroporation
Na_V channel	voltage-gated Na^+ channel
QTc interval	corrected QT interval

References

- Hong, C.M.; Liu, C.H.; Su, T.H.; Yang, H.C.; Chen, P.J.; Chen, Y.W.; Kao, J.H.; Liu, C.J. Real-world effectiveness of direct-acting antiviral agents for chronic hepatitis C in Taiwan: Real-world data. *J. Microbiol. Immunol. Infect.* **2020**, *53*, 569–577. [[CrossRef](#)] [[PubMed](#)]
- Panahi, Y.; Gorabi, A.M.; Talaie, S.; Beiraghdar, F.; Akbarzadeh, A.; Tarhriz, V.; Mellatyar, H. An overview on the treatments and prevention against COVID-19. *Virol. J.* **2023**, *20*, 23. [[CrossRef](#)] [[PubMed](#)]
- Ackerman, M.J.; Clapham, D.E. Ion channels—Basic science and clinical disease. *N. Engl. J. Med.* **1997**, *336*, 1575–1586. [[CrossRef](#)] [[PubMed](#)]
- Franciolini, F. Patch clamp technique and biophysical study of membrane channels. *Experientia* **1986**, *42*, 589–594. [[CrossRef](#)] [[PubMed](#)]
- Kausar, S.; Said Khan, F.; Ishaq Mujeeb Ur Rehman, M.; Akram, M.; Riaz, M.; Rasool, G.; Hamid Khan, A.; Saleem, I.; Shamim, S.; Malik, A. A review: Mechanism of action of antiviral drugs. *Int. J. Immunopathol. Pharmacol.* **2021**, *35*, 20587384211002621. [[CrossRef](#)] [[PubMed](#)]
- Chen, T.S.; Lai, M.C.; Huang, H.I.; Wu, S.N.; Huang, C.W. Immunity, Ion Channels and Epilepsy. *Int. J. Mol. Sci.* **2022**, *23*, 6446. [[CrossRef](#)]
- Zhu, S.; Wang, J.; Wang, Y.; Chu, J.; Liu, Y.; Chen, X.; Chen, X. QTc prolongation during antiviral therapy in two COVID-19 patients. *J. Clin. Pharm. Ther.* **2020**, *45*, 1190–1193. [[CrossRef](#)] [[PubMed](#)]
- Santoro, F.; Monitillo, F.; Raimondo, P.; Lopizzo, A.; Brindicci, G.; Gilio, M.; Musaico, F.; Mazzola, M.; Vestito, D.; Benedetto, R.D.; et al. QTc Interval Prolongation and Life-Threatening Arrhythmias During Hospitalization in Patients with Coronavirus Disease 2019 (COVID-19): Results From a Multicenter Prospective Registry. *Clin. Infect. Dis.* **2021**, *73*, e4031–e4038. [[CrossRef](#)]
- Esmel-Vilomara, R.; Dolader, P.; Sabaté-Rotes, A.; Soriano-Arandes, A.; Gran, F.; Rosés-Noguer, F. QTc interval prolongation in patients infected with SARS-CoV-2 and treated with antiviral drugs. *An. Pediatr. (Engl. Ed.)* **2022**, *96*, 213–220. [[CrossRef](#)]
- Hu, C.H.; Wu, S.N.; So, E.C. Tyrosine kinase inhibitors, ionic currents, and cardiac arrhythmia. *Front. Oncol.* **2023**, *13*, 1218821. [[CrossRef](#)]
- Qiao, G.; Li, S.; Yang, B.; Li, B. Inhibitory effects of artemisinin on voltage-gated ion channels in intact nodose ganglion neurones of adult rats. *Basic Clin. Pharmacol. Toxicol.* **2007**, *100*, 217–224. [[CrossRef](#)] [[PubMed](#)]

12. So, E.C.; Wu, S.N.; Wu, P.C.; Chen, H.Z.; Yang, C.J. Synergistic Inhibition of Delayed Rectifier K⁺ and Voltage-Gated Na⁺ Currents by Artemisinin in Pituitary Tumor (GH3) Cells. *Cell. Physiol. Biochem.* **2017**, *41*, 2053–2066. [[CrossRef](#)]
13. Zhang, D.; Atochina-Vasserman, E.N.; Lu, J.; Maurya, D.S.; Xiao, Q.; Liu, M.; Adamson, J.; Ona, N.; Reagan, E.K.; Ni, H.; et al. The Unexpected Importance of the Primary Structure of the Hydrophobic Part of One-Component Ionizable Amphiphilic Janus Dendrimers in Targeted mRNA Delivery Activity. *J. Am. Chem. Soc.* **2022**, *144*, 4746–4753. [[CrossRef](#)]
14. Liu, Y.-C.; So, E.C.; Wu, S.-N. Cannabidiol Modulates M-Type K⁺ and Hyperpolarization-Activated Cation Currents. *Biomedicines* **2023**, *11*, 2651. [[CrossRef](#)] [[PubMed](#)]
15. Wu, S.N.; Huang, H.C.; Yeh, C.C.; Yang, W.H.; Lo, Y.C. Inhibitory effect of memantine, an NMDA-receptor antagonist, on electroporation-induced inward currents in pituitary GH3 cells. *Biochem. Biophys. Res. Commun.* **2011**, *405*, 508–513. [[CrossRef](#)] [[PubMed](#)]
16. Tsai, K.L.; Chang, H.F.; Wu, S.N. The inhibition of inwardly rectifying K⁺ channels by memantine in macrophages and microglial cells. *Cell. Physiol. Biochem.* **2013**, *31*, 938–951. [[CrossRef](#)]
17. Wang, C.L.; Tsai, M.L.; Wu, S.N. Evidence for mitoxantrone-induced block of inwardly rectifying K⁺ channels expressed in the osteoclast precursor RAW 264.7 cells differentiated with lipopolysaccharide. *Cell. Physiol. Biochem.* **2012**, *30*, 687–701. [[CrossRef](#)]
18. Shiau, A.L.; Lee, K.H.; Cho, H.Y.; Chuang, T.H.; Yu, M.C.; Wu, C.L.; Wu, S.N. Molnupiravir, a ribonucleoside antiviral prodrug against SARS-CoV-2, alters the voltage-gated sodium current and causes adverse events. *Virology* **2023**, *587*, 109865. [[CrossRef](#)] [[PubMed](#)]
19. Chang, W.T.; Liu, P.Y.; Lee, K.; Feng, Y.H.; Wu, S.N. Differential Inhibitory Actions of Multitargeted Tyrosine Kinase Inhibitors on Different Ionic Current Types in Cardiomyocytes. *Int. J. Mol. Sci.* **2020**, *21*, 1672. [[CrossRef](#)]
20. Amarh, E.; Tisdale, J.E.; Overholser, B.R. Prolonged Exposure to Remdesivir Inhibits the Human Ether-A-Go-Go-Related Gene Potassium Current. *J. Cardiovasc. Pharmacol.* **2023**, *82*, 212–220. [[CrossRef](#)]
21. Cho, H.Y.; Chuang, T.H.; Wu, S.N. Effective Perturbations on the Amplitude and Hysteresis of Erg-Mediated Potassium Current Caused by 1-Octylnonyl 8-[(2-hydroxyethyl)[6-oxo-6(undecyloxy)hexyl]amino]-octanoate (SM-102), a Cationic Lipid. *Biomedicines* **2021**, *9*, 1367. [[CrossRef](#)] [[PubMed](#)]
22. Wu, S.N.; Yeh, C.C.; Wu, P.Y.; Huang, H.C.; Tsai, M.L. Investigations into the correlation properties of membrane electroporation-induced inward currents: Prediction of pore formation. *Cell Biochem. Biophys.* **2012**, *62*, 211–220. [[CrossRef](#)] [[PubMed](#)]
23. Chang, W.T.; Liu, P.Y.; Gao, Z.H.; Lee, S.W.; Lee, W.K.; Wu, S.N. Evidence for the Effectiveness of Remdesivir (GS-5734), a Nucleoside-Analog Antiviral Drug in the Inhibition of I (K(M)) or I (K(DR)) and in the Stimulation of I (MEP). *Front. Pharmacol.* **2020**, *11*, 1091. [[CrossRef](#)] [[PubMed](#)]
24. Li, Y. Qinghaosu (artemisinin): Chemistry and pharmacology. *Acta Pharmacol. Sin.* **2012**, *33*, 1141–1146. [[CrossRef](#)]
25. Ho, W.E.; Peh, H.Y.; Chan, T.K.; Wong, W.S. Artemisinins: Pharmacological actions beyond anti-malarial. *Pharmacol. Ther.* **2014**, *142*, 126–139. [[CrossRef](#)]
26. Fuzimoto, A.D. An overview of the anti-SARS-CoV-2 properties of *Artemisia annua*, its antiviral action, protein-associated mechanisms, and repurposing for COVID-19 treatment. *J. Integr. Med.* **2021**, *19*, 375–388. [[CrossRef](#)] [[PubMed](#)]
27. de Oliveira, J.R.; Antunes, B.S.; do Nascimento, G.O.; Kawall, J.C.S.; Oliveira, J.V.B.; Silva, K.; Costa, M.A.T.; Oliveira, C.R. Antiviral activity of medicinal plant-derived products against SARS-CoV-2. *Exp. Biol. Med.* **2022**, *247*, 1797–1809. [[CrossRef](#)] [[PubMed](#)]
28. Urban, N.; Schaefer, M. Direct Activation of TRPC3 Channels by the Antimalarial Agent Artemisinin. *Cells* **2020**, *9*, 202. [[CrossRef](#)] [[PubMed](#)]
29. Dillard, L.K.; Fullerton, A.M.; McMahan, C.M. Ototoxic hearing loss from antimalarials: A systematic narrative review. *Travel Med. Infect. Dis.* **2021**, *43*, 102117. [[CrossRef](#)]
30. Peng, T.; Li, S.; Liu, L.; Yang, C.; Farhan, M.; Chen, L.; Su, Q.; Zheng, W. Artemisinin attenuated ischemic stroke induced cell apoptosis through activation of ERK1/2/CREB/BCL-2 signaling pathway in vitro and in vivo. *Int. J. Biol. Sci.* **2022**, *18*, 4578–4594. [[CrossRef](#)]
31. Fraguas-Sánchez, A.I.; Torres-Suárez, A.I. Medical Use of Cannabinoids. *Drugs* **2018**, *78*, 1665–1703. [[CrossRef](#)] [[PubMed](#)]
32. van Breemen, R.B.; Muchiri, R.N.; Bates, T.A.; Weinstein, J.B.; Leier, H.C.; Farley, S.; Tafesse, F.G. Cannabinoids Block Cellular Entry of SARS-CoV-2 and the Emerging Variants. *J. Nat. Prod.* **2022**, *85*, 176–184. [[CrossRef](#)] [[PubMed](#)]
33. Marquez, A.B.; Vicente, J.; Castro, E.; Vota, D.; Rodríguez-Varela, M.S.; Lanza Castronuovo, P.A.; Fuentes, G.M.; Parise, A.R.; Romorini, L.; Alvarez, D.E.; et al. Broad-Spectrum Antiviral Effect of Cannabidiol Against Enveloped and Nonenveloped Viruses. *Cannabis Cannabinoid Res.* **2023**, ahead of print.
34. Viudez-Martínez, A.; García-Gutiérrez, M.S.; Manzanares, J. Cannabidiol regulates the expression of hypothalamus-pituitary-adrenal axis-related genes in response to acute restraint stress. *J. Psychopharmacol.* **2018**, *32*, 1379–1384. [[CrossRef](#)] [[PubMed](#)]
35. Huang, C.W.; Lin, P.C.; Chen, J.L.; Lee, M.J. Cannabidiol Selectively Binds to the Voltage-Gated Sodium Channel Na(v)1.4 in Its Slow-Inactivated State and Inhibits Sodium Current. *Biomedicines* **2021**, *9*, 1141. [[CrossRef](#)]
36. Sankaranarayanan, S.; Simasko, S.M. Characterization of an M-like current modulated by thyrotropin-releasing hormone in normal rat lactotrophs. *J. Neurosci.* **1996**, *16*, 1668–1678. [[CrossRef](#)] [[PubMed](#)]
37. Varghese, N.; Moscoso, B.; Chavez, A.; Springer, K.; Ortiz, E.; Soh, H.; Santaniello, S.; Maheshwari, A.; Tzingounis, A.V. KCNQ2/3 Gain-of-Function Variants and Cell Excitability: Differential Effects in CA1 versus L2/3 Pyramidal Neurons. *J. Neurosci.* **2023**, *43*, 6479–6494. [[CrossRef](#)] [[PubMed](#)]

38. Simasko, S.M.; Sankaranarayanan, S. Characterization of a hyperpolarization-activated cation current in rat pituitary cells. *Am. J. Physiol.* **1997**, *272*, E405–E414. [[CrossRef](#)] [[PubMed](#)]
39. Chen, C.S.; So, E.C.; Wu, S.N. Modulating Hyperpolarization-Activated Cation Currents through Small Molecule Perturbations: Magnitude and Gating Control. *Biomedicines* **2023**, *11*, 2177. [[CrossRef](#)] [[PubMed](#)]
40. Arvanitakis, Z.; Shah, R.C.; Bennett, D.A. Diagnosis and Management of Dementia: Review. *JAMA* **2019**, *322*, 1589–1599. [[CrossRef](#)]
41. Pereira, A.; Santos, I.A.; da Silva, W.W.; Nogueira, F.A.R.; Bergamini, F.R.G.; Jardim, A.C.G.; Corbi, P.P. Memantine hydrochloride: A drug to be repurposed against Chikungunya virus? *Pharmacol. Rep.* **2021**, *73*, 954–961. [[CrossRef](#)]
42. Butterworth, R.F. Adamantanes for the treatment of neurodegenerative diseases in the presence of SARS-CoV-2. *Front. Neurosci.* **2023**, *17*, 1128157. [[CrossRef](#)] [[PubMed](#)]
43. Müller, T.; Riederer, P.; Kuhn, W. Aminoadamantanes: From treatment of Parkinson’s and Alzheimer’s disease to symptom amelioration of long COVID-19 syndrome? *Expert Rev. Clin. Pharmacol.* **2023**, *16*, 101–107. [[CrossRef](#)] [[PubMed](#)]
44. Cheek, E.R.; Fast, V.G. Nonlinear changes of transmembrane potential during electrical shocks: Role of membrane electroporation. *Circ. Res.* **2004**, *94*, 208–214. [[CrossRef](#)] [[PubMed](#)]
45. Dyachok, O.; Zhabyeyev, P.; McDonald, T.F. Electroporation-induced inward current in voltage-clamped guinea pig ventricular myocytes. *J. Membr. Biol.* **2010**, *238*, 69–80. [[CrossRef](#)] [[PubMed](#)]
46. Hibino, H.; Inanobe, A.; Furutani, K.; Murakami, S.; Findlay, I.; Kurachi, Y. Inwardly rectifying potassium channels: Their structure, function, and physiological roles. *Physiol. Rev.* **2010**, *90*, 291–366. [[CrossRef](#)] [[PubMed](#)]
47. Eklund, J.; Kozloff, M.; Vlamakis, J.; Starr, A.; Mariott, M.; Gallot, L.; Jovanovic, B.; Schilder, L.; Robin, E.; Pins, M.; et al. Phase II study of mitoxantrone and ketoconazole for hormone-refractory prostate cancer. *Cancer* **2006**, *106*, 2459–2465. [[CrossRef](#)] [[PubMed](#)]
48. Preet, G.; Oluwabusola, E.T.; Milne, B.F.; Ebel, R.; Jaspars, M. Computational Repurposing of Mitoxantrone-Related Structures against Monkeypox Virus: A Molecular Docking and 3D Pharmacophore Study. *Int. J. Mol. Sci.* **2022**, *23*, 14287. [[CrossRef](#)]
49. Kitamura, H.; Yokoyama, M.; Akita, H.; Matsushita, K.; Kurachi, Y.; Yamada, M. Tertiapin potently and selectively blocks muscarinic K⁺ channels in rabbit cardiac myocytes. *J. Pharmacol. Exp. Ther.* **2000**, *293*, 196–205. [[PubMed](#)]
50. Vignani, F.; Bertaglia, V.; Buttigliero, C.; Tucci, M.; Scagliotti, G.V.; Di Maio, M. Skeletal metastases and impact of anticancer and bone-targeted agents in patients with castration-resistant prostate cancer. *Cancer Treat. Rev.* **2016**, *44*, 61–73. [[CrossRef](#)]
51. Stojilkovic, S.S.; Tabak, J.; Bertram, R. Ion channels and signaling in the pituitary gland. *Endocr. Rev.* **2010**, *31*, 845–915. [[CrossRef](#)]
52. Sanderson, T.; Hisner, R.; Donovan-Banfield, I.A.; Hartman, H.; Løchen, A.; Peacock, T.P.; Ruis, C. A molnupiravir-associated mutational signature in global SARS-CoV-2 genomes. *Nature* **2023**, *623*, 594–600. [[CrossRef](#)] [[PubMed](#)]
53. Zarenezhad, E.; Marzi, M. Review on molnupiravir as a promising oral drug for the treatment of COVID-19. *Med. Chem. Res.* **2022**, *31*, 232–243. [[CrossRef](#)] [[PubMed](#)]
54. Wu, S.N.; So, E.C.; Liao, Y.K.; Huang, Y.M. Reversal by ranolazine of doxorubicin-induced prolongation in the inactivation of late sodium current in rat dorsal root ganglion neurons. *Pain Med.* **2015**, *16*, 1032–1034. [[CrossRef](#)] [[PubMed](#)]
55. Salazar, C.A.; Basilio Flores, J.E.; Veramendi Espinoza, L.E.; Mejia Dolores, J.W.; Rey Rodriguez, D.E.; Loza Munárriz, C. Ranolazine for stable angina pectoris. *Cochrane Database Syst. Rev.* **2017**, *2*, Cd011747. [[CrossRef](#)] [[PubMed](#)]
56. Cardoso, F.C.; Lewis, R.J. Sodium channels and pain: From toxins to therapies. *Br. J. Pharmacol.* **2018**, *175*, 2138–2157. [[CrossRef](#)]
57. Gordon, C.J.; Tchesnokov, E.P.; Feng, J.Y.; Porter, D.P.; Götte, M. The antiviral compound remdesivir potently inhibits RNA-dependent RNA polymerase from Middle East respiratory syndrome coronavirus. *J. Biol. Chem.* **2020**, *295*, 4773–4779. [[CrossRef](#)] [[PubMed](#)]
58. Morse, J.S.; Lalonde, T.; Xu, S.; Liu, W.R. Learning from the Past: Possible Urgent Prevention and Treatment Options for Severe Acute Respiratory Infections Caused by 2019-nCoV. *Chembiochem* **2020**, *21*, 730–738. [[CrossRef](#)]
59. Sheahan, T.P.; Sims, A.C.; Leist, S.R.; Schäfer, A.; Won, J.; Brown, A.J.; Montgomery, S.A.; Hogg, A.; Babusis, D.; Clarke, M.O.; et al. Comparative therapeutic efficacy of remdesivir and combination lopinavir, ritonavir, and interferon beta against MERS-CoV. *Nat. Commun.* **2020**, *11*, 222. [[CrossRef](#)] [[PubMed](#)]
60. Spinner, C.D.; Gottlieb, R.L.; Criner, G.J.; Arribas López, J.R.; Cattelan, A.M.; Soriano Viladomiu, A.; Ogbuagu, O.; Malhotra, P.; Mullane, K.M.; Castagna, A.; et al. Effect of Remdesivir vs Standard Care on Clinical Status at 11 Days in Patients with Moderate COVID-19: A Randomized Clinical Trial. *JAMA* **2020**, *324*, 1048–1057. [[CrossRef](#)]
61. Wang, M.; Cao, R.; Zhang, L.; Yang, X.; Liu, J.; Xu, M.; Shi, Z.; Hu, Z.; Zhong, W.; Xiao, G. Remdesivir and chloroquine effectively inhibit the recently emerged novel coronavirus (2019-nCoV) in vitro. *Cell Res.* **2020**, *30*, 269–271. [[CrossRef](#)]
62. Grundeis, F.; Ansems, K.; Dahms, K.; Thieme, V.; Metzendorf, M.I.; Skoetz, N.; Benstoem, C.; Mikolajewska, A.; Griesel, M.; Fichtner, F.; et al. Remdesivir for the treatment of COVID-19. *Cochrane Database Syst. Rev.* **2023**, *1*, Cd014962. [[PubMed](#)]
63. Beigel, J.H.; Tomashek, K.M.; Dodd, L.E.; Mehta, A.K.; Zingman, B.S.; Kalil, A.C.; Hohmann, E.; Chu, H.Y.; Luetkemeyer, A.; Kline, S.; et al. Remdesivir for the Treatment of COVID-19—Final Report. *N. Engl. J. Med.* **2020**, *383*, 1813–1826. [[CrossRef](#)] [[PubMed](#)]
64. Pilote, S.; Simard, C.; Drolet, B. Remdesivir (VEKLURY) for Treating COVID-19: Guinea Pig Ex Vivo and In Vivo Cardiac Electrophysiological Effects. *J. Cardiovasc. Pharmacol.* **2022**, *80*, 616–622. [[CrossRef](#)] [[PubMed](#)]
65. Fung, J.S.; Levitan, M.; Landry, S.; Mclsaac, S. Torsades de pointes associated with remdesivir treatment for COVID-19 pneumonia. *J. Assoc. Med. Microbiol. Infect. Dis. Can.* **2023**, *8*, 99–104. [[CrossRef](#)] [[PubMed](#)]

66. Tchesnokov, E.P.; Feng, J.Y.; Porter, D.P.; Götte, M. Mechanism of Inhibition of Ebola Virus RNA-Dependent RNA Polymerase by Remdesivir. *Viruses* **2019**, *11*, 326. [[CrossRef](#)] [[PubMed](#)]
67. Nabati, M.; Parsaee, H. Potential Cardiotoxic Effects of Remdesivir on Cardiovascular System: A Literature Review. *Cardiovasc. Toxicol.* **2022**, *22*, 268–272. [[CrossRef](#)]
68. Brown, A.J.; Won, J.J.; Graham, R.L.; Dinnon, K.H., 3rd; Sims, A.C.; Feng, J.Y.; Cihlar, T.; Denison, M.R.; Baric, R.S.; Sheahan, T.P. Broad spectrum antiviral remdesivir inhibits human endemic and zoonotic deltacoronaviruses with a highly divergent RNA dependent RNA polymerase. *Antiviral Res.* **2019**, *169*, 104541. [[CrossRef](#)] [[PubMed](#)]
69. Hassett, K.J.; Benenato, K.E.; Jacquinet, E.; Lee, A.; Woods, A.; Yuzhakov, O.; Himansu, S.; Deterling, J.; Geilich, B.M.; Ketova, T.; et al. Optimization of Lipid Nanoparticles for Intramuscular Administration of mRNA Vaccines. *Mol. Ther. Nucleic Acids* **2019**, *15*, 1–11. [[CrossRef](#)]
70. Lam, K.; Leung, A.; Martin, A.; Wood, M.; Schreiner, P.; Palmer, L.; Daly, O.; Zhao, W.; McClintock, K.; Heyes, J. Unsaturated, Trialkyl Ionizable Lipids are Versatile Lipid-Nanoparticle Components for Therapeutic and Vaccine Applications. *Adv. Mater.* **2023**, *35*, e2209624. [[CrossRef](#)]
71. Naidu, G.S.; Yong, S.B.; Ramishetti, S.; Rampado, R.; Sharma, P.; Ezra, A.; Goldsmith, M.; Hazan-Halevy, I.; Chatterjee, S.; Aitha, A.; et al. A Combinatorial Library of Lipid Nanoparticles for Cell Type-Specific mRNA Delivery. *Adv. Sci.* **2023**, *10*, e2301929. [[CrossRef](#)]
72. Behr, J.P.; Demeneix, B.; Loeffler, J.P.; Perez-Mutul, J. Efficient gene transfer into mammalian primary endocrine cells with lipopolyamine-coated DNA. *Proc. Natl. Acad. Sci. USA* **1989**, *86*, 6982–6986. [[CrossRef](#)] [[PubMed](#)]
73. Albert, E.; Aurigemma, G.; Saucedo, J.; Gerson, D.S. Myocarditis following COVID-19 vaccination. *Radiol. Case Rep.* **2021**, *16*, 2142–2145. [[CrossRef](#)] [[PubMed](#)]
74. Bozkurt, B.; Kamat, I.; Hotez, P.J. Myocarditis with COVID-19 mRNA Vaccines. *Circulation* **2021**, *144*, 471–484. [[CrossRef](#)] [[PubMed](#)]
75. Kim, H.W.; Jenista, E.R.; Wendell, D.C.; Azevedo, C.F.; Campbell, M.J.; Darty, S.N.; Parker, M.A.; Kim, R.J. Patients with Acute Myocarditis following mRNA COVID-19 Vaccination. *JAMA Cardiol.* **2021**, *6*, 1196–1201. [[CrossRef](#)] [[PubMed](#)]
76. Vidula, M.K.; Ambrose, M.; Glassberg, H.; Chokshi, N.; Chen, T.; Ferrari, V.A.; Han, Y. Myocarditis and Other Cardiovascular Complications of the mRNA-Based COVID-19 Vaccines. *Cureus* **2021**, *13*, e15576. [[CrossRef](#)] [[PubMed](#)]
77. Williams, C.B.; Choi, J.I.; Hosseini, F.; Roberts, J.; Ramanathan, K.; Ong, K. Acute Myocarditis Following mRNA-1273 SARS-CoV-2 Vaccination. *CJC Open* **2021**, *3*, 1410–1412. [[CrossRef](#)] [[PubMed](#)]
78. Cho, H.Y.; Chuang, T.H.; Wu, S.N. The Effectiveness in Activating M-Type K⁺ Current Produced by Solifenacin ([[(3R)-1-azabicyclo[2.2.2]octan-3-yl] (1S)-1-phenyl-3,4-dihydro-1H-isoquinoline-2-carboxylate): Independent of Its Antimuscarinic Action. *Int. J. Mol. Sci.* **2021**, *22*, 12399. [[CrossRef](#)] [[PubMed](#)]
79. Martín-Montañez, E.; López-Téllez, J.F.; Acevedo, M.J.; Pavía, J.; Khan, Z.U. Efficiency of gene transfection reagents in NG108-15, SH-SY5Y and CHO-K1 cell lines. *Methods Find. Exp. Clin. Pharmacol.* **2010**, *32*, 291–297. [[CrossRef](#)] [[PubMed](#)]
80. Azdaki, N.; Farzad, M. Long QT interval and syncope after a single dose of COVID-19 vaccination: A case report. *Pan Afr. Med. J.* **2021**, *40*, 67. [[CrossRef](#)]
81. Abdelgalil, A.A.; Alkahtani, H.M.; Al-Jenoobi, F.I. Sorafenib. *Profiles Drug Subst. Excip. Relat. Methodol.* **2019**, *44*, 239–266.
82. Cabrera, R.; Limaye, A.R.; Horne, P.; Mills, R.; Soldevila-Pico, C.; Clark, V.; Morelli, G.; Firpi, R.; Nelson, D.R. The anti-viral effect of sorafenib in hepatitis C-related hepatocellular carcinoma. *Aliment. Pharmacol. Ther.* **2013**, *37*, 91–97. [[CrossRef](#)] [[PubMed](#)]
83. Lin, C.S.; Huang, S.H.; Yan, B.Y.; Lai, H.C.; Lin, C.W. Effective Antiviral Activity of the Tyrosine Kinase Inhibitor Sunitinib Malate against Zika Virus. *Infect. Chemother.* **2021**, *53*, 730–740. [[CrossRef](#)] [[PubMed](#)]
84. Theerawatanasirikul, S.; Lueangaramkul, V.; Semkum, P.; Lekcharoensuk, P. Antiviral mechanisms of sorafenib against foot-and-mouth disease virus via c-RAF and AKT/PI3K pathways. *Vet. Res. Commun.* **2023**, *48*, 329–343. [[CrossRef](#)]
85. Kloth, J.S.; Pagani, A.; Verboom, M.C.; Malovini, A.; Napolitano, C.; Kruit, W.H.; Sleijfer, S.; Steeghs, N.; Zambelli, A.; Mathijssen, R.H. Incidence and relevance of QTc-interval prolongation caused by tyrosine kinase inhibitors. *Br. J. Cancer* **2015**, *112*, 1011–1016. [[CrossRef](#)] [[PubMed](#)]
86. Sung, R.J.; Kuo, C.-T.; Wu, S.-N.; Lai, W.-T.; Luqman, N.; Chan, N.-Y. Sudden cardiac death syndrome: Age, gender, ethnicity, and genetics. *Acta Cardiol. Sin.* **2008**, *24*, 65–74.
87. Anson, L.; Briviba, M.; Silamikelis, I.; Terentjeva, A.; Perkons, I.; Birzniece, L.; Rovite, V.; Rozentale, B.; Viksna, L.; Kolesova, O.; et al. Amino Acid Metabolism is Significantly Altered at the Time of Admission in Hospital for Severe COVID-19 Patients: Findings from Longitudinal Targeted Metabolomics Analysis. *Microbiol. Spectr.* **2021**, *9*, e0033821. [[CrossRef](#)]

Disclaimer/Publisher's Note: The statements, opinions and data contained in all publications are solely those of the individual author(s) and contributor(s) and not of MDPI and/or the editor(s). MDPI and/or the editor(s) disclaim responsibility for any injury to people or property resulting from any ideas, methods, instructions or products referred to in the content.